Reactive and Functional Polymers 196 (2024) 105843

Contents lists available at ScienceDirect

Reactive and Functional Polymers

journal homepage: www.elsevier.com/locate/react

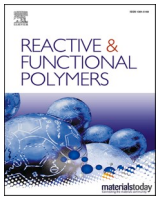

Zwitterionic stabilized water-borne polymer colloids for antifouling coatings

Sumi Murali [a], Amaia Agirre [a], Jon Arrizabalaga [a], Iliane Rafaniello [a], Thomas Schäfer [a,b], Radmila Tomovska [a,b,*]

[a] POLYMAT, Kimika Aplikatua saila, Kimika Fakultatea, Universidad del País Vasco/Euskal Herriko Unibertsitatea UPV/EHU, Joxe Mari Korta zentroa, Tolosa hiribidea, 72, 20018 Donostia, Spain
[b] IKERBASQUE, Basque Foundation for Science, Bilbo, Spain

ARTICLE INFO

Keywords:
Zwitterionic monomers
Waterborne (meth)acrylic coatings
Emulsifier-free emulsion polymerization
Protein adsorption
Antifouling coatings

ABSTRACT

This study presents antifouling waterborne (meth)acrylic coatings prepared through seeded semi-continuous emulsion polymerization, using trace amounts of a zwitterionic monomer 2-(methacryloyloxy)ethyl dimethyl-(3-sulfopropyl)ammonium hydroxide (DMAPS). DMAPS was introduced with a dual purpose, to establish a protective layer of DMAPS containing polymer chains on the films' surface, thereby imparting antifouling characteristics, while simultaneously provides in-situ colloidal stability to the emulsion during polymerization.

By providing colloidal stability to (meth)acrylic polymer particles in aqueous dispersion (latex), DMAPS-rich units are distributed on the surface of the polymer particles and subsequently on the surface of the resulting polymer films. Subsequent analysis revealed that the films exhibited diminished hydrophilicity, a more textured surface, and diminished affinity for water entrapment compared to conventionally stabilized (meth)acrylic films. Such surfaces demonstrated high resistance to fouling and weak adhesion of the studied BSA protein. These effects were positively influenced by the quantity of DMAPS incorporated within the (meth)acrylic films that allow higher coverage with DMAPS rich polymer chains.

The proposed methodology not only emphasizes a potent pathway for the development of environmentally-conscious, waterborne film-forming coating technology but also involves the simultaneous integration of a zwitterionic surface layer, conveying remarkable antifouling attributes to the resulting (meth)acrylic coating film.

1. Introduction

Polymers containing ionic groups in their structure are among the most important classes of macromolecules. Unlike to polyelectrolytes that present either positive or negative charges, or polyampholytes that have both charges in different monomeric units, zwitterionic polymers (also known as polybetaines) present opposite charges in each repeating unit. The cationic group is usually quaternary ammonioum, whereas the anionic one can be sulfonic (SO_3^-), phosphonic (PO_4^-) or carboxylic (COO^-), classifying the zwitterionic polymers as sulfo-, phospho- or carboxy-betaines, respectively [1,2].

The balance of opposite charges in the polymer structure brings to the polyzwitterions unique characteristics of overall charge neutrality, high hydrophilicity, electrostatic interactions, antifouling and anti-polyelectrolyte behaviour, which unlock a range of application possibilities, including non-fouling coatings [3,4], drug-delivery systems [5], membranes [6,7], etc. Concerning the antifouling capability, even it has been quite deeply studied for polyzwitterions, there are not clear rules to predict their antifouling efficiency and the mechanism remains still unrevealed [8]. Commonly, the antifouling mechanism is explained by a water barrier layer formation on the surface of the film that reduces significantly the adsorption of the protein (foulant) due to steric repulsions. Therefore, hydrophilic polymers, such as polyethylene glycol (PEG) for example, have been extensively used as a gold standard in non-fouling surfaces, through a formation of H-bonds with the water molecules [9–12]. However, the H-bonds are not strong enough and may break quite easily. On the contrary, the water layer formed on the zwitterionic polymer films is more tightly bonded due to the

* Corresponding author at: POLYMAT, Kimika Aplikatua saila, Kimika Fakultatea, Universidad del País Vasco/Euskal Herriko Unibertsitatea UPV/EHU, Joxe Mari Korta zentroa, Tolosa hiribidea, 72, 20018 Donostia, Spain.
E-mail address: radmila.tomovska@ehu.eus (R. Tomovska).

https://doi.org/10.1016/j.reactfunctpolym.2024.105843
Received 16 October 2023; Received in revised form 26 December 2023; Accepted 29 January 2024
Available online 30 January 2024
1381-5148/© 2024 The Authors. Published by Elsevier B.V. This is an open access article under the CC BY-NC-ND license (http://creativecommons.org/licenses/by-nc-nd/4.0/).

electrostatically induced strong hydration [13–15], thus, are more suitable candidate for long-term antifouling properties. Among all, sulfobetaines, 2-(methacryloyloxy) ethyl dimethyl-(3-sulfopropyl) ammonium hydroxide (DMAPS) has been extensively studied for its excellent antifouling properties.[7,16–19.]

In many studies aimed at enhancing antifouling properties, the surfaces have been typically modified using zwitterionic (co)polymers. This can be achieved through methods such as grafting zwitterionic polymers to create polyzwitterion brushes [16,17,18,19] or by coating the substrate surface with a copolymer containing zwitterionic units [6,7,20]. However, one significant limitation for practical applications is that the production of zwitterionic monomers is not straightforward, and these monomers are still costly products. This cost factor poses a challenge in the widespread adoption of zwitterionic coatings and materials despite their potential antifouling benefits.

On the other hand, water-borne emulsion polymers are essential industrial products with environmental friendly nature, with production for of about 35 million tones/year in 2021 with clear growing trend, only for coating application [21]. However, the typical water-borne polymers are prone to easy fouling, which limits their applications for protection in harsh environments, such as marine for example. This brings an idea of their combination, or even better, to add small amount of zwitterionic monomers to film-forming water-borne polymer coating formulations and to produce coating protective films able to protect the surfaces against fouling. Such a strategy will bring a robustness to the coating films covered by zwitterionic units and widen significantly their applications.

Recently, we have demonstrated that DMAPS can be used as an alternative to conventional surfactants in industrial-like emulsion polymerization, to produce (meth)acrylic film-forming polymer dispersions (latexes) [22]. This strategy allowed in-situ incorporation of DMAPS onto the polymer particles surface in water-borne dispersion, providing colloidal stability and conveying mechanical reinforcement and increased water resistance to the resulting coating films [22]. Motivated by the good antifouling properties of DMAPS containing films, in this work the effect of the surface presence of DMAPS onto polymer particles over antifouling characteristics of the coating film was studied. To the best of the authors' knowledge, this is the first study of antifouling properties of films cast from zwitterionic monomer containing water-borne polymer dispersions. For that aim, polymer latexes were prepared by seeded semicontinuous emulsion polymerization of n-butyl acrylate/methyl methacrylate (MMA/BA, 50:50 weight ratio) using different amounts of DMAPS. The antifouling properties were tested by evaluating the bovine serum albumin (BSA) protein adsorption on the films containing different amounts of DMAPS, studied by quartz crystal microbalance with dissipation monitoring (QCM-D) and by multi parametric surface plasmon resonance (MP-SPR) in a PBS buffer.

The present work present promising strategy towards antifouling coatings with clear economic and environmental advantages. Owing to the employed emulsion polymerization process of low-cost acrylic monomers, it can easily be scaled up, and due to the replacement of organic solvents by water during synthesis, it enables environmentally friendly coatings. Final and most important advantage would be the straightforward incorporation of very small quantity of zwitterionic units that will grant powerful antifouling protection to the final film.

2. Experimental

2.1. Materials

The monomers methyl methacrylate (MMA, purity 99.9%, Quimidroga), n-butyl acrylate (n-BA, purity 99.5%, 10–20 ppm MEHQ, Quimidroga), butyl methacrylate (BMA, Sigma-Aldrich) and zwitterionic monomer 2-(methacryloyloxy) ethyl dimethyl-(3-sulfopropyl) ammonium hydroxide (DMAPS) (purity≥95.0%, Sigma-Aldrich) were used. The chemical structure of DMAPS is shown in Scheme 1. The initiator

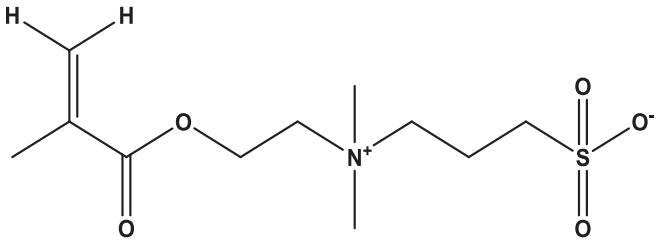

Scheme 1. Chemical structure of DMAPS

potassium persulfate (KPS, Aldrich), the components of redox initiator system (oxidant tert-butyl hydroperoxide, TBHP, 70 wt% aqueous solution, Luperox from Sigma-Aldrich, and reductant Bruggolite (FF7) (Bruggemann), and the conventional surfactant sodium dodecyl sulfate (SDS, Sigma-Aldrich) were used without any purification. As continuous medium for emulsion preparation, distilled water was utilized through this work. Hydroquinone (HQ, purity, 99%, Panreac) was employed to stop the reactions.

2.2. Polymerizations

The polymer latexes were prepared by a seeded semi-continuous emulsion polymerization method. The seed used in all syntheses was prepared in batch emulsion polymerization of MMA/n-BA with 50/50 weight ratio, 10% solids content, SDS emulsifier (2 wt% related to the monomers) and KPS thermal initiator (1 wt% realted to the monomers).

In the semi continuous process, appropriate seed quantity was placed in a reactor, in which the main monomers n-BA and MMA in a 50/50 weight ratio in pre-emulsion were slowly fed throughout the whole polymerization process. The TBHP/FF7 redox couple initiator with a concentration of 1% based on the weight of the monomer was used to initiate the reactions. The pre-emulsion was prepared by emulsifying the monomers in water in presence of either DMAPS or SDS and FF7. The concentration of DMAPS was either 2 or 5 wt% with respect to the main monomers quantity, whereas the reference latex was synthesized with 2 wt% SDS. Target solids content was 50 wt%. Before introducing the pre-emulsion, the oxidant TBHP was added to the reactor as a shot. Additional information regarding the polymerization process can be found elsewhere [22].

On the other hand, in order to confirm the anti-polyelectrolyte behaviour of the latex stabilized with DMAPS, another two latexes were synthesized (Table 1) with solids content of 10%. In one of them, water was used as a continuous phase and in the other, an aqueous solution of 0.02 M NaCl.

The polymerization reactions were performed in a 1 L jacketed glass reactor equipped with reflux condenser, N_2 inlet, temperature probe, stainless steel agitator and a sampling tube. The reactor was first charged with an aqueous solution of DMAPS and monomer BMA under stirring (200 rpm). The redox pair initiator was added semicontinuously during 1.5 h. The aqueous solutions of reductant (FF7) and oxidant (TBHP) were fed separately into the reactor for 90 min at a temperature of 70 °C. Afterwards, the reaction was left at the same temperature to proceed batch-wise for 3.5 h under stirring.

Table 1
Recipe for the latex synthesized in the presence and absence of NaCl (10% S.C.)

Ingredients	Wt (%)	Amount (g)
BMA	9.9	80.03
ZMs *	0.2	1.62
TBHP *	0.1	0.81
FF7	0.1	1.14
Water/0.02 M NaCl	90	720.48

* weight based to BMA (butyl methacrylate) monomer (wbm).

2.3. Characterization

The conversion of volatile monomers (MMA, n-BA) was determined gravimetrically. Approximately, 1 mL latex samples were withdrawn from the reactor and transferred into aluminium (Al) pans having 1–2 drops of hydroquinone aqueous solution (1 wt% in water). The aliquots in Al pans were kept for 2–3 h in the fume hood, and then dried in the oven at 60 °C overnight. The conversion of DMAPS for the final latexes was determined by using ^{1}H NMR Spectroscopy (Bruker Avance-400), for that aim 450 μL of the final latex were dissolved in 50 μL D_2O.

Z-average particle diameter was measured at 25 °C by dynamic light scattering (DLS), using Malvern ZetaSizer Nano-S instrument equipped with a 633 nm red laser. For particle diameter, the samples withdrawn from the reactor were diluted with MiliQ water to prevent multiple scattering. For the *Z*-potential, the same Malvern ZetaSizer Nano-S instrument was used and the samples were diluted with MiliQ water. Particle size distribution was determined by capillary hydrodynamic fractionation in a CHDF-3000 instrument (Matec Applied Sciences). The samples were run at a carrier flow rate of 1.4 mL/min at 35 °C (1/4 GR 500 carrier from Matec). The incorporation of DMAPS was determined by FTIR (Bruker Alpha FTIR spectrometer with ATR mode). Analyses were performed on polymer films prepared from original (non-dialysed) latex and dialysed latex, assuming that all DMAPS that was not incorporated onto MMA/n-BA particles was removed during dialysis. This means that the film prepared from such latex would contain only DMAPS incorporated onto polymer particles. Films were introduced in the sample holder and average of five measurements were taken. Spectra were recorded in transmission mode in the spectral region from 4000 to 400 cm^{-1} with a resolution of 0.9 cm^{-1}. The area of the peak of sulfonate group (1035 cm^{-1}) was used to prepare a calibration curve from films with known DMAPS concentration.

Stability of latexes towards electrolyte addition was studied by adding equal amount of saline solution into the latex. The saline solutions were prepared with different concentrations of NaCl (0.5, 0.75, and 1 M) and $CaCl_2$ (1 M). After shaking them properly, they were allowed to rest for 24 h, afterwards the particle size was measured by DLS.

Particle size of latexes with DMAPS in the presence and absence of salt was determined by TEM using Jeol TM-1400 Plus series 120Kv electron microscope. The latex were diluted with deionized water and placed on copper grids covered with Formaver R and dried at ambient temperatures.

To prepare the films for characterization, the latexes were cast either on glass substrates (for contact angle measurements, film thickness 120 μm) and silicone molds and dried at 23 °C and 55% relative humidity until constant weight for the film was obtained. In order to eliminate the effect of the S.C. on the film quality prior to film casting, all the latex were diluted to 30% S.C.

A standard sessile drop method was employed to determine the static water contact angle on the films' surface. Data Physics OCA 20 model goniometer was utilized for that aim. A water drop (3 μL deionized water) was placed on the films and an average of minimum 10 measurements taken from different locations on the surface was reported.

The surface morphology of the films was investigated by Atomic Force Microscopy (AFM) measurements were performed, using a Bruker dimension icon atomic force microscope equipped with the NanoScope V Controller (Bruker), operating in tapping mode. An integrated silicon tip/cantilever (TESP-V2, Bruker) with a resonance frequency of 320 kHz and nominal constant of 37 N/m was used.

Water (moisture) permeability (P) of the films was measured by a gravimetric cell (Sartorius BP210D) in order to determine the ability of the films as humidity barrier coatings. The cell was a small container of Teflon that was partially filled with water and sealed by a polymeric membrane. 300 μm thick films were then attached to the open mouth of the gravimetric cell containing water so that the film is exposed to water vapour (100% relative humidity). The cell was well sealed so that the water could only escape by permeating through the film and it was placed on a balance within a temperature-controlled chamber (25 °C) to measure the loss of weight during time. The moisture permeability (g mm/m^2 day) was calculated from the slope of the weight loss (water loss) versus time plot by using Eq. 1.

$$P = \mathrm{m}\, f/A\ (\mathrm{a}_{int} - \mathrm{a}_{ext}) \tag{1}$$

where m is the slope of the curve, f is the film thickness, A is the area of contact between the film and water vapour (2.54 cm^2), a_{int} is the water vapour activity in the headspace of the cell (considered 1) and a_{ext} is the water vapour activity in the chamber. Three samples of each films were tested.

To detect the antifouling ability of the films, quartz crystal microbalance with dissipation monitoring (QCM-D) was used, using bovine serum albumin (BSA) as model foulant. QCM-D measurements were performed on a Q-SENSE E1 system operating at 23 °C. The latexes were deposited by means of drop-coating with 2 μL pipette and dried at room temperature for three days. Prior to the measurements, the samples were stabilized overnight under a constant PBS buffer flux of 100 μL /min. Subsequently, they were put in contact with different concentrations of BSA in aqueous buffer (PBS) solution up to a maximum of 1000 mg BSA/L. QCM-D technique detects changes in the resonance frequency (Δf), and dissipation (ΔD). During the adsorption/desorption cycle, the resonance frequency of the crystal changes according to changes in the mass. If the mass forms an evenly distributed, rigid layer whose mass is small compared to that of the crystal, then the mass per unit area can be calculated from the Sauerbrey equation.

$$\Delta \mathrm{m} = -\mathrm{C}\cdot\Delta \mathrm{f}/\mathrm{n} \tag{2}$$

In this equation, C is a constant (17.7 ng cm^{-2} s^{-1} for this equipment) and n is the resonance overtone number ($n = 5$ was used here). Where appropriate, a 2nd order data noise smoothing was applied for better visualization of the data.

Prior to carrying out surface plasmonic resonance measurments, the MP-SPR SiO_2 sensor was first introduced in an ozone cleaner for 10 min. Then, the sensor was placed in a sensor holder and introduced in a beaker with Milli-Q water for at least another 10 min. Afterwards, the sensor was dried with nitrogen and placed in the support for SPR sensors. Then a measurement of 30 s was carried out (in gas range) in order to get the reference peak minimum angle of the SPR curve. Afterwards, the sensor was placed on the spin coater (kept in place by applying vacum) and 5 μL of the latex (0.03 wt%) were deposited on the sensor and left to dry in the oven (50 °C) overnight. Once the film was completely dry it was stabilized with a phosphate buffer solution (PBS) for several hours (at least 5 h). Once the sensor was stabilized adsorption measurement were carried out. First, 10 min baseline was made as reference with PBS buffer. Then, BSA 1000 ppm solution was passed over the sensor for 65 min (adsorption) and finally, PBS buffer was injected for at least another 60 min (desorption).

3. Results and discussions

3.1. Characteristics of latexes

Before analysing the obtained results, it is worth describing how colloidal stabilization in emulsion polymerization of MMA/n-BA proceeds when using DMAPS instead of conventional emulsifiers, as reported in our previous work [22]. In the absence of the emulsifier, the stabilizing units are created in situ by the chemical incorporation of DMAPS into MMA/BA chains. However, this is a challenging task due to the high hydrophilicity of DMAPS and the high hydrophobicity of MMA/BA.

Thus, copolymerization occurs with the MMA/n-BA solubilized in the aqueous phase of the emulsion after adding a water-soluble free-radical thermal initiator. The oligoradicals created in this way gain

sufficient hydrophobicity through the addition of more MMA/BA units and then enter into the MMA/n-BA particles. Nevertheless, these oligoradicals can terminate in the aqueous phase, leading to the formation of water-soluble oligomers that negatively influence colloidal stability and polymer properties.

To maximize the incorporation of DMAPS onto particles and minimize the creation of soluble oligomers, reaction-engineering strategies are employed. This includes slowly feeding the MMA and n-BA monomers into the reactor, maintaining their concentration low, while maximizing the concentration of DMAPS. Additionally, the formation of hydrophobic radicals in the aqueous phase reduces the time that each oligoradical spends in the aqueous phase, thereby decreasing the probability of premature termination before they enter the polymer particles.

Following this methodology, two colloidally stable latexes (aqueous polymer dispersions) were synthesized with 2 and 5% DMAPS. ^{1}H NMR spectra of the polymer produced with 2% DMAPS are shown in Supporting information (Fig. S1), demonstrating that the polymer contains all added monomers: DMAPS (5.7 ppm), BA (1.4 ppm) and MMA (3.7 ppm). By increasing DMAPS concentration from 2% to 5%, the average particle size decreased from 275 nm to 236 nm, respectively, probably due to higher concentration of stabilizing units at higher DMAPS concentration, approaching the particle size of the reference latex synthesized using conventional surfactant SDS (243 nm). In contrast to the reference and 2% DMAPS latexes, the 5% DMAPS latex presented about 15% of coagulum, likely induced by the high ionic strength in this dispersion, a consequence of the higher fraction of water-soluble oligomers. After the coagulum removal the amount of DMAPS incorporated was 1.01 g (50.6%) per 100 g polymer in the case of 2% DMAPS and more than doubled 2.2 g (44.4%) per 100 g of polymer for the latex stabilized with 5% DMAPS. The fraction of DMAPS that was not incorporated onto particles was included in the water-soluble oligomers, which indeed is higher in case of 5% DMAPS. Even though we tried to determine this fraction by latex centrifugation and aqueous phase analysis, due to the strong ionic interactions, it was difficult to separate all the soluble oligomers, giving rise to inconsistent results.

Colloidal stability of ionically stabilized polymer particles in latex is determined by a balance of two opposing forces: electrostatic repulsion and attractive Van der Waals forces. When colloids approach each other, their electrical double layer (EDL) maximizes repulsion, but this force weakens beyond the EDL, while simultaneously, attractive forces increase. Adding salts to the dispersions usually compresses the EDL by interacting with its ions. This enhances attractive particle forces and often leads to coagulation. Latexes with higher colloidal stability will experience delayed coagulation at higher salt concentrations.

Therefore, the colloidal stability of the latexes containing DMAPS was evaluated by addition of salts with different concentration, followed by measuring the particle size prior and after salt addition (Fig. 1). Since DMAPS was not fully incorporated onto the polymer particles, the latex synthesized with 2% DMAPS was dialysed to remove the water-soluble species and to study how their presence affects the salt stability. In addition, since all the latexes were synthesized by seeded semi-continuous emulsion polymerization using SDS stabilized seed, the excess surfactant is also removed during dialysis.

From Fig. 1, it can be clearly seen that under the addition of different concentrations of NaCl, all the latexes, including the reference latex, maintained colloidal stability. However, with increasing NaCl concentration, there was a significant increase in the particle size of the latexes with 2% DMAPS, which moreover coagulated when 1 M $CaCl_2$ was added. The dialyzed counterpart of the 2% latex showed slightly improved stability in the presence of NaCl, although at 1 M $CaCl_2$, the ionic strength was already too high, resulting in coagulation as well. This indicates that the 2% latex is still sensitive to salt addition, possibly due to the insufficient concentration of stabilizing polymer chains.

The presence of water-soluble species in the latex has a negative effect on colloidal stability. Considering that Ca2+ is a divalent cation, whereas Na + is monovalent, under the same salt concentrations, $CaCl_2$ provides a higher ion quantity and ionic strength. Conversely, when the 5% DMAPS latex was exposed to the same salts and concentration, there was no change in particle size observed, even after the addition of 1 M $CaCl_2$. The incorporation of a higher quantity of DMAPS in the 5% latex likely resulted in an increased concentration of stabilizing chains, maintaining colloidal stability even at very high ionic strengths.

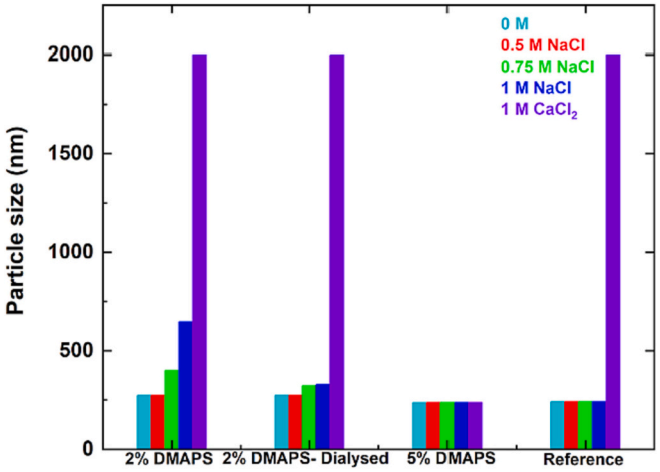

Fig. 1. Salt stability of the latexes synthesized with 2 and 5% DMAPS, 2% DMAPS after dialysis and reference latex.

Moreover, in the 5% DMAPS latex, it is assumed that most of the DMAPS-containing soluble oligomers were removed from the dispersions within the coagulum. This latex presented improved colloidal stability compared to the reference, probably because of the compression of the electric double layer (EDL) at higher ionic strengths in the reference. Conversely, the DMAPS-containing chains in the 5% DMAPS latex, after salt addition, likely extended towards the aqueous phase, improving colloidal stability (anti-polyelectrolyte effect), as shown in Fig. 2a.

In the polymer latex, due to the high hydrophilicity of DMAPS, the polymer chains rich in DMAPS are located on the surface of the polymer particles, providing colloidal stability to MMA/n-BA particles. Due to the interactions of the added salt ions with the zwitterions, the inter- and intra-molecular interactions in the DMAPS-containing chains were disrupted, inducing chain extensions. In this way, the distance between the particles is kept larger, preventing the coagulation of the latex.

To verify if there is anti-polyelectrolyte effect occurring in the latexes, the synthesis of a latex with 2% DMAPS was performed in a presence and absence of salt (0.02 M NaCl) and the corresponding particle size was measured by DLS (Table 2), determining the hydrodynamic diameter and by TEM (Fig. 2b and c), analysing the particles in a dry state.

As shown in Table 2, the DLS measurements clearly indicates that particle size was increased in the latex synthesized in salt presence due to the anti-polyelectrolyte effect. Therefore, the particle size determined by DLS is larger than in the latex obtained in absence of salt. The findings are consistent with those reported by Polzer et al. [23], who observed an increase in the thickness of the grafted DMAPS brush onto PS crosslinked particles at high NaCl concentrations. Nevertheless, the particle size of both latexes was similar when measured by TEM (Fig. 2a and b, respectively), where the intrinsic particle diameter can be observed. More careful observation of the TEM images shows that, besides the dry collapsed state of the particles, distinctions between the particle morphology can still be appreciated. The salt-free original latex (Fig. 2b) exhibited a well-defined core-shell structure, where the core is made of MMA/n-BA, while the shell is rich in DMAPS. The shell is thin and well-defined, corresponding to the collapsed state of the DMAPS rich polymer chains due to inter- and intra- molecular interactions. In Fig. 2c on the other hand, in a presence of salt, there is no clear border between the

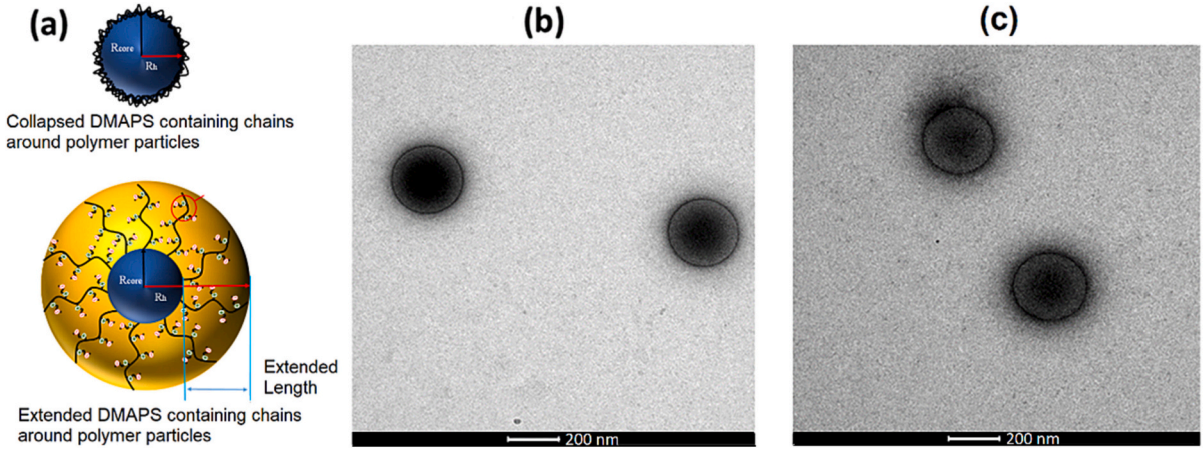

Fig. 2. (a) Schematic representation of MMA/n-BA polymer particles stabilized by DMAPS containing chains, in absence of salt (top) and in presence of salt (bottom); TEM images of surfactant-free latex in the absence of salt (b) and in the presence of salt (c).

Table 2
Particle size of surfactant free latex in the presence and absence of salt.

Latex	DLS	TEM
	Dp (nm)	Dp (nm)
2% DMAPS in the absence of salt	234	242
2% DMAPS in the presence of salt	320	258

core and shell, which is larger. Moreover, around the particles an extension might be appreciated. If this extension is considered, the particle size would correspond to that determined by DLS (320 nm). This change can be attributed to the extension of DMAPS polymer chains on the particle surface, which could stretch further away from the core, resulting in a corrugation of the shell.

These results confirmed the presence of anti-polyelectrolyte effect in the DMAPS stabilized latexes, which probably is the main reason for the improved salt stability of the latex which contain enough DMAPS containing stabilizing chains.

3.2. Characteristics of films

Polymer films were prepared from the latexes by water evaporation under standard atmospheric conditions. Because the MMA/n-BA latexes prepared in this work are film forming, continuous and transparent films were obtained. Mechanical properties of these films as well as their water sensibility are reported elsewhere [22]. The water contact angles measured on the films' surface are presented in Fig. 3, showing that the contact angle of the films containing DMAPS is higher than that of the reference film, indicating less hydrophilic films. The reason behind this could be twofold, on one hand due to the migration of the conventional surfactant SDS during film formation [24,25], it accumulates on the surface of the reference film making it more hydrophilic. On the other hand, the drop of hydrophilicity of the films containing DMAPS might arise because of the possible lack of the migration of any species, but also due to a neutralization effect of the ionically bonded zwitterions, similar to what was observed by Argaiz et al. [26] In addition, Azzaroni et al. [27] also reported similar contact angles for DMAPS brushes grafted on silicone surfaces. They attributed these high contact angles to a super collapsed state arising from the high number on inter and intra chain polymer interactions. When these interactions were disrupted by increasing the temperature above the upper critical solubility temperature (UCST), the surface turned to be very hydrophilic (C.A. $\sim 10^{\circ}$).

The surface morphology was analysed by AFM imaging, and phase images of the film surface are shown in Fig. 4. Presence of large white aggregates arising from the SDS migration towards the film-air interface

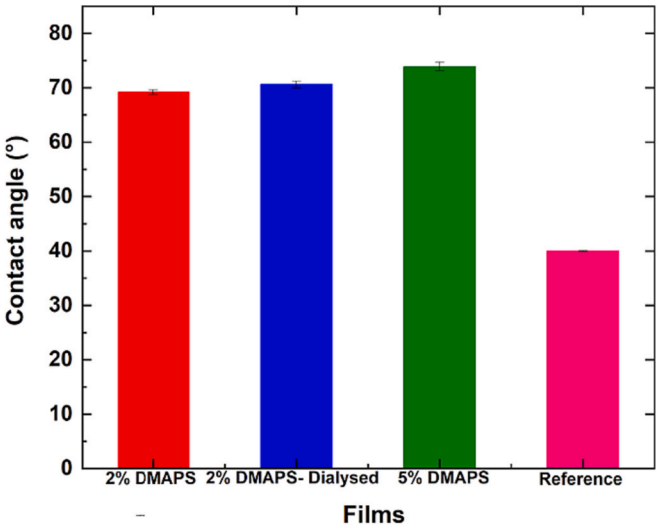

Fig. 3. Contact angle of a drop of water on the films cast from the latex synthesized with different DMAPS concentrations, 2% DMAPS after dialysis and reference.

during film formation can be clearly appreciated in the reference film (Fig. 4a). They introduced the strong hydrophilicity observed at the surface of the reference film by contact angle measurements. The presence of whitish structures in the DMAPS containing films (Fig. 4b to d) are attributed to the small quantity of SDS coming from the seed. This quantity is the less on the surface of dialysed 2% DMAPS film (Fig. 4c), because most of the SDS was removed when 2% DMAPS latex was dialysed. On the other hand, the amount of SDS observed on the surface of 5% DMAPS film was much lower than for 2% DMAPS film, because large coagulum quantity was removed from this latex prior to film formation. We assumed that most of the soluble species, including SDS were placed within the coagulum.

It is well known that the roughness of the film also has important impact to the antifouling properties [28], therefore, the height AFM images of the films' surface were also analysed (Fig. 5). The rough surface is considered favourable to improve the fouling behaviour, however, it has been reported that the roughness of the surface coated with zwitterionic polymer brushes is reduced when the film is immersed in water [29,30,31]. The smoother surface created would reduce the antifouling arising from the roughness. In Fig. 5, the height scale bar presented in each of the images determines the maximum peak to valley

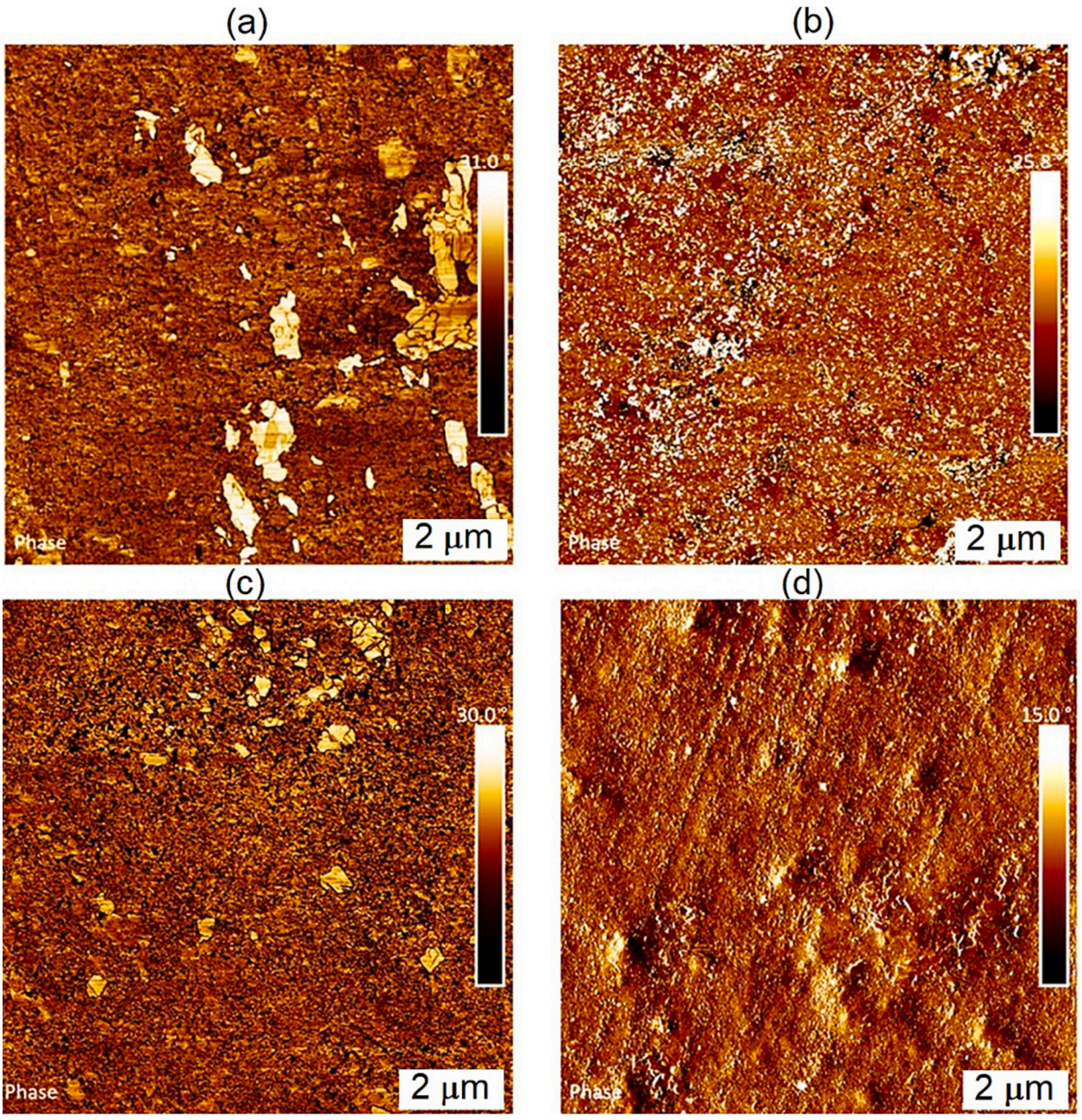

Fig. 4. AFM phase images of film-air interfaces of (a) reference; (b) 2% DMAPS; (c) 2% DMAPS dialysed; (d) 5% DMAPS.

height over the sample. The absolute values between the highest and lowest points along to the colour difference of the film surface were used to compare the roughness of the different films. According to these criteria, the reference film (Fig. 5a) is quite rough; probably the irregular surface was created by the distributed SDS aggregates with different sizes over the film surface. On the other hand, the both 2% DMAPS films original and dialysed (Fig. 5b and c) are the smoothest one, whereas the most irregular and rough surface is that of 5% DMAPS film (Fig. 5d). The roughness trend does not correspond to the trend in the contact angles observed in Fig. 6. Nevertheless, the DMAPS films being less hydrophilic by chemical nature and ionic complexation process, are secondary affected by the roughness that might further increase the contact angle.

The humidity barrier properties are important for protective coatings. They were determined by measuring humidity permeation, which happen in three consecutive steps. First, the film absorbs the vapour, which then diffuses through the film from which it is finally desorbed. In our previous work [22], it was found that by the use of 2% of DMAPS the moisture permeation was reduced one order of magnitude with respect to the reference. It was thought that the presence of an ionic complex network (honeycomb network distributed all over the MMA/n-BA matrix), made of chains rich in DMAPS introduces physical obstacles to the diffusion of water through the film. This network was formed during film formation from the chains rich in DMAPS placed on the surface of MMA/n-BA particles for their colloidal stabilization. Nevertheless, when this network was destroyed by annealing of the film (as observed in AFM images) [22], the water barrier properties of the film were not changed. Since during heating of the film above its glass transition temperature, the polymer chains got increased mobility, the ionic complexation likely was further promoted by the improved contact between the zwitterions. We hypothesized that the enhanced humidity barrier might be related rather with the ionic complexation within the whole film that decreased the hydrophilicity than with the ionic complex network. If so, higher is

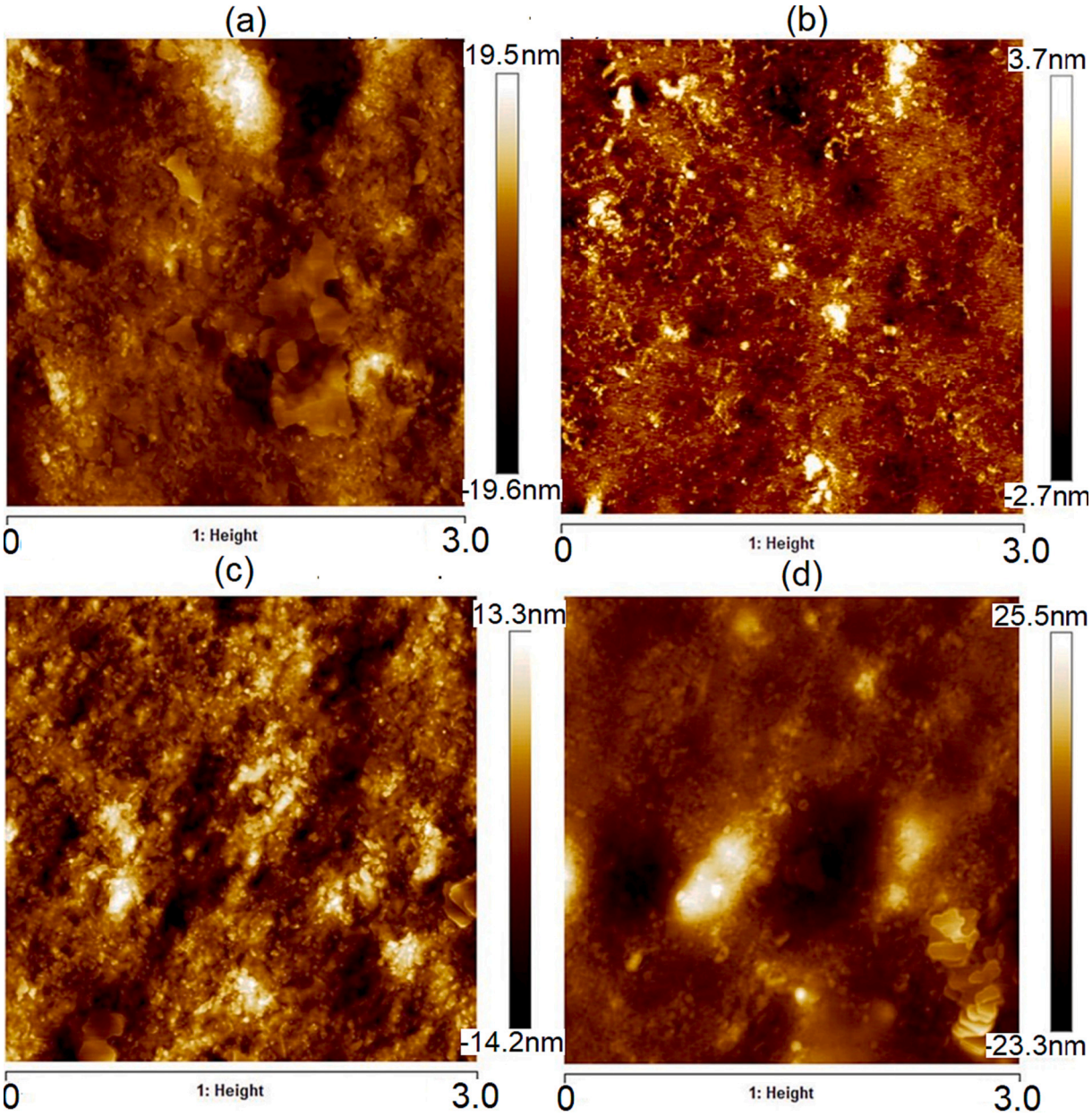

Fig. 5. AFM height images of film-air interfaces of (a) reference film; (b) 2% DMAPS; (c) 2% DMAPS dialysed; and (d) 5% DMAPS.

the amount of DMAPS within the film, lower would be the moisture permeation. The water vapour barrier of the present films is shown in Fig. 6. Indeed, the humidity barrier is significantly enhanced for the DMAPS containing films than for the reference, however, oppositely to what was expected, the water vapour barrier was almost not affected by the amount of DMAPS. The best performance was obtained by the 2% dialysed film, likely due to the latex dialysis prior to film formation, in which process the water-soluble species presented in the latex including SDS were removed, therefore, the hydrophilic pathways for humidity diffusion were also removed.

3.3. Antifouling properties of films

BSA was the selected protein to evaluate the capability of the films for protein adsorption. Under aqueous conditions, the zwitterionic moieties arising from DMAPS are expected to be oriented to the aqueous phase giving negative surface charge as suggested by the zeta potential measurements [22]. In the same way, under the PBS buffer solution employed during the experiment (pH = 7.4) the protein might be strongly negatively charged favouring the repellence between the protein and substrate. The same interactions are expecting to happen in the case of reference latex, which is negatively charged due to SDS reach surface.

Even though in literature [32–34] the excellent anti-fouling characteristics of zwitterionic polymer coatings are explained by the electrostatically induced hydration layer by the high density ions, the water contact angles present in Fig. 3 indicates that DMAPS films are less hydrophilic than the reference and probably less prone to form hydrating layers. In order to determine the antifouling properties of the polymer films, BSA adsorption on the four polymer films including reference was evaluated by QCM-D studies. Both the change in frequency (Δf) and dissipation (ΔD) were monitored over time (Fig. 7a and b, respectively). It can be observed in Fig. 7a that all the films, including the reference show relatively low protein adsorption. Nevertheless, the reference film presents the largest Δf, fivefold that of DMAPS containing films. Between the DMPAS containing films, that with 5% DMAPS

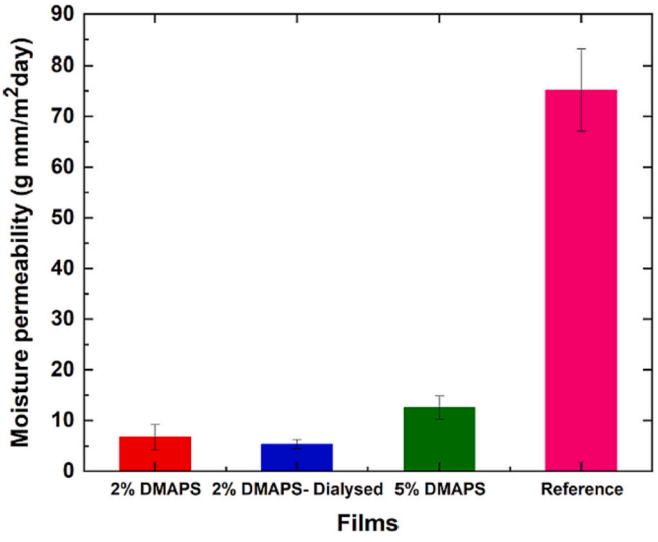

Fig. 6. Water vapour permeability of films containing 2% DMAPS (prior and after dialysis), film containing 5% DMAPS and reference film.

adsorbed the least protein quantity, less than both original and dialysed 2% DMAPS films. In addition, there was no significant difference between 2% DMAPS original and dialysed, which was quite surprising, due to the lower concentration of DMAPS in the dialysed 2% DMAPS. Likely, the DMAPS concentration on the surface of the film was not affected by the dialysis process, which is related to the lack of migration of DMAPS containing water soluble oligomers towards film-air surface during film formation [22].

The change in the dissipation, shown in Fig. 17b, is the largest for 5% DMAPS film, whereas the reference shows the lowest dissipation, indicating that the protein is more rigidly and permanently attached to the reference surface, whereas the BSA on the 5% DMAPS film surface is weakly and reversibly adsorbed.

Nevertheless, it should be taken into account that QCM-D determines both the adsorbed BSA and its associated water ("wet mass"). Therefore, in order to shed a bit of light on the matter, the films were analysed by MP- SPR and the results are shown in Fig. 8. In contrast to QCM-D that determines the frequency change due to adsorbed amount of material, MP-SPR is an optical technique that measures the change in the refractive index. Therefore the detected values are exclusively due to protein adsorption, and do not cover the water absorbed by the film (it determines the "dry mass"). Fig. 8 also shows that the reference film present the highest BSA adsorption, whereas the 5% DMAPS film the lowest one. Taking into account that the antifouling character arises from the presence of DMAPS, these results are in agreement with the expected ones since higher is DMAPS concentration in the film, lower is the BSA adsorption.

However, in contrast to the QCM-D and as expected, MP-SPR results mark a clear difference between the BSA adsorption on the 2% DMAPS original film and the dialyzed one. The BSA adsorption on the 2% DMAPS dialyzed film is very similar to that of the reference, probably due to the reduction of DMAPS amount in the film after dialysis with respect to the non-dialyzed. While dialyzing the latex, all the water-soluble oligomers presenting smaller molecular sizes than the pore size of the membrane are removed from the latex and subsequently from the film. In this way, the DMAPS that was not incorporated onto the polymer particles (50%) would be removed, resulting in a film with lower amount of DMAPS.

To understand the results better, the approximate surface masses for both, QCM-D and MP-SPR results were calculated (Table 3). For the approximation of the adsorbed mass determined by QCM-D, Sauerbrey equation was used (Eq. 2). This equation is a linear relationship between the resonance frequency changes of an oscillating quartz crystal and its surface mass changes and it is defined as follows:

$$\Delta m = 17.7 \bullet \Delta f \tag{3}$$

where, Δf is the resonance frequency change (Hz), Δm is the surface mass of the adsorbed layer (ng/cm^2) and, 17.7 ng/cm^2 Hz is a constant comprising sensor specific characteristic parameters.

On the other hand, for the SPR results, a linear relationship between peak minimum angle change in the SPR and its surface mass changes was used to approximately calculate the BSA adsorbed on the surface of the film, presented by Eq. 4.

$$\Delta m = 0,8333 \bullet \Delta\theta \tag{4}$$

where, $\Delta\theta$ is the peak minimum angle change (mdeg), Δm is the surface mass of the added layer (ng/cm^2). 0.8333 ng/cm^2 mdeg is a constant, which approximately correlates the change in angle to the change in surface mass for a measurement wavelength of 670 nm.

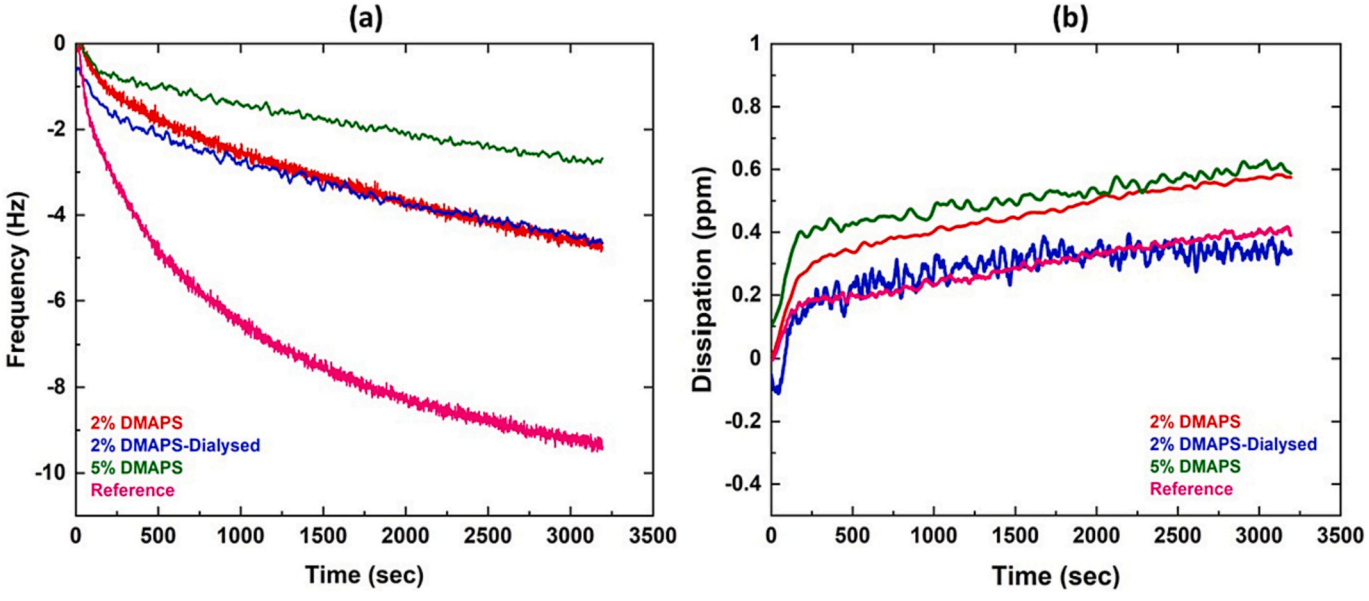

Fig. 7. QCM-D results, (a) frequency change; and (b) dissipation profiles with time of polymer films exposed to BSA in PBS solution.

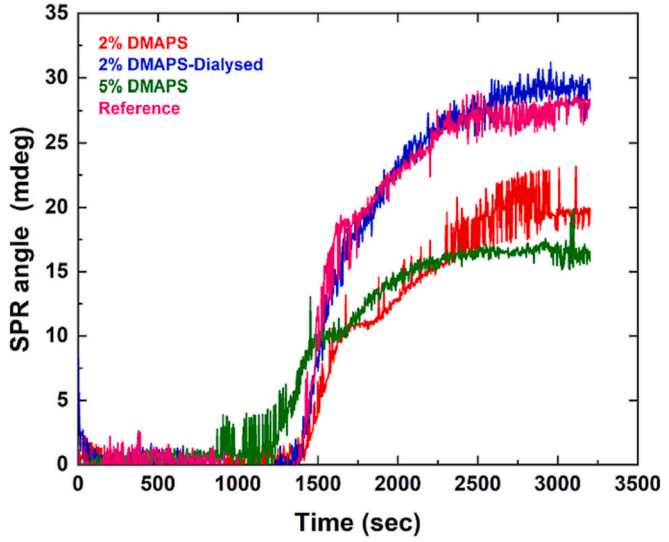

Fig. 8. MP-SPR adsorption of BSA on sensors prepared by depositing a film from different latexes.

Table 3
Amount of BSA adsorbed on the different films calculated by Eqs. 2 and 3 from QCM-D results and Eq. 4 from MP-SPR results, and the amount of associated water.

BSA adsorbed	mQCM-D [ng/cm^2]	mMP-SPR [ng/cm^2]	Associated water in QCM-D [ng/cm^2]
2% DMAPS	80	16	64
2% DMAPS (dialysed)	80	24	56
5% DMAPS	44	14	30
Reference	168	23	145

The resulting surface masses in ng/cm^2 together with the amount of associated water calculated from the difference between the measured BSA adsorption by QCM-D and MP-SPR are presented in Table 3.

Table 3 shows that the surface masses determined by MP-SPR were significantly (3–7 times) lower than the same measured by QCM-D, clearly demonstrating that the QCM-D results encompass both the BSA and the water adsorption. On the other hand, it is clear that the reference film adsorbed 3-fold higher water quantity than the DMAPS containing films, for which the associated water quantity dropped with increasing DMAPS content. Interestingly, 2% dialysed DMAPS contains less DMAPS than original 2% DMAPS and presents less amount of associative water. The difference might be because of the SDS removal during the dialysis, which make the difference in their hydrophilicity. The quantity of BSA adsorbed follows similar trend, thus 5% DMAPS film seems to be less prone to fouling. These results are in concordance with the tendency in hydrophilicity shown in Fig. 3, according to which 5% DMAPS is the less hydrophilic, supported also by the lowest associated water quantity in Table 3.

Considering that in the literature the antifouling capacity of the polymer film surface is related with the capability of the film to associate water and form a thicker hydrophilic layer that prevent protein adsorption on the film, along to the strength of the water molecules bonding, these results indicate that there is another phenomenon happening that affects the antifouling behaviour.

5% DMAPS film is the least hydrophilic according to the CA measurements and associative water on this film is the lowest, demonstrating that the water film created on the surface of this film will be the thinnest in comparison to the other DMAPS containing films and the reference one, in accordance to the associated water quantity (Table 3). On the other hand, as AFM images shown (Fig. 8) this film is the roughest one, which capture the water molecules more stable once bounded strongly on the surface. Since the protein are also strongly hydrophilic, having the thinner water layer surrounding the film, less proteins would have access to the film. Due to strongly, electrostatically bound water, stabilized moreover by the rougher surface rich in DMAPS units, there will be less free adsorption sites for the protein adsorption. On the contrary, there is a thicker associative water layer created on the reference film that can be an efficient medium to bring more proteins to the film. The water molecules are weakly bound on the surface and might easily be replaced by the BSA molecules. Another effect rarely investigated in the literature is a coverage of the film surface with the DMAPS units. Taking into consideration that in 5% DMAPS film there is a double DMAPS quantity (incorporation is 2.2 g per 100 g of polymer) than in 2% DMAPS film (1 g per 100 g polymer), it is clear that for higher DMAPS quantity in the films, higher is the coverage of the surface, which results in less original MMA/n-BA film will interact with the protein. This is probably an additional parameter that affects the fouling behaviour and explains the observed differences in the BSA adsorption.

On the other hand, the QCM-D results shows that the 5% DMAPS film presented the highest dissipation indicating a more viscoelastic attachment between the protein and the film surface whereas, the reference presented the lowest dissipation as an indicative of a more rigid attachment between the BSA and the surface of the film. As explained before the change in dissipation can be related with the associative water, and usually for higher associative water quantity, higher is the dissipation. However, the associative water amounts presented in Table 3 showed the opposite trend, being the reference with the highest amount of associative water and the 5% DMAPS with the lowest. Furthermore, the trend observed in the amount of associative water was in agreement with the water-uptake results presented in the previous work [22], where it was found that the water absorption decreased as DMAPS concentration in the film increased. Similar results were found by Bengani et al. [7] where they found that the swelling for the co-polymers containing low amount of DMAPS was negligible due to the low interconnectivity between DMAPS domains. Even more, when the water-uptake was repeated for the 2% DMAPS after dialysis the water-uptake decreased even more as so did the amount of associative water (Table 3). Therefore, it seems that the higher dissipation observed by the QCM-D on the films with increased DMAPS content clearly can be related to a weaker adsorption. A possible consequence could be that regeneration (removal of BSA adsorbed) of DMAPS 5% film could be easier than with the reference sample. A schematic representation of the effect of DMAPS concentration on the BSA adsorption on the films with different DMAPS coverage is given in Fig. 9.

4. Conclusions

In this work, the antifouling capability of waterborne coating film based on MMA/n-BA film forming formulation was studied, in which the colloidal stability was provided by incorporation of small quantity of zwitterionic monomer DMAPS (2 and 5 wt% with respect to MMA/n-BA). The distribution of DMAPS on the surface of polymer particles, and subsequently on the film surface was expected to convey capability of hydrating the film, bounding strongly a water layer that will protect it against fouling.

Colloidally stable polymer dispersions – latexes were obtained, with average particle size in a range of 236–275 nm, and excellent salt-stability due to demonstrated anti-polyelectrolyte effect. According to this effect, the DMAPS containing chains extended in salted aqueous dispersions, improving the colloidal stability.

The surface of the DMAPS containing polymer films were less hydrophilic, rougher and finally much less prone to fouling than the reference one, stabilized with conventional surfactant SDS. The least fouling surface was provided by the film containing 5% DMAPS, for

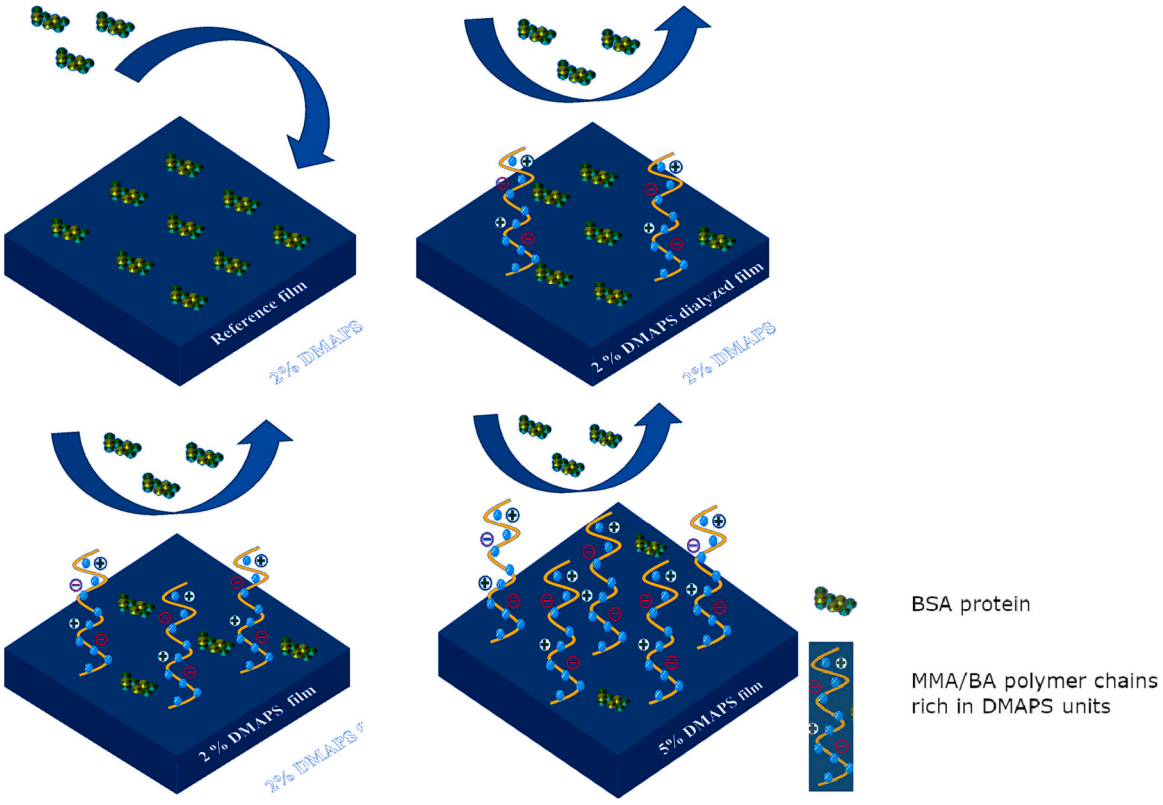

Fig. 9. Schematic representation of the effect of DMAPS concentration on the antifouling of BSA; Annotation is added on the right of the image.

which it was found that associated the least water quantity, however bound strongly due to both electrostatic interactions and rougher surface. This behaviour is opposite than reported for antifouling activities of DMAPS surfaces, according to which the thicker is the associative water layer lower is the protein adsorption. These findings indicate other parameters that affects the protein adsorption, likely related to the coverage of the surface of the film with DMAPS units on one hand and the strength of the water bounding that will determine the possibility of the protein bonding.

The findings of this work introduce a new light to the antifouling behaviour of the zwitterionic surfaces and could be useful for the design of such surface for different applications, not limited to the coating applications targeted in this work.

CRediT authorship contribution statement

Sumi Murali: Data curation, Formal analysis, Investigation, Visualization, Writing – original draft. **Amaia Agirre:** Conceptualization, Methodology, Supervision, Writing – review & editing. **Jon Arrizabalaga:** Formal analysis, Investigation, Visualization. **Iliane Rafaniello:** Formal analysis, Investigation, Visualization. **Thomas Schäfer:** Conceptualization, Methodology, Supervision. **Radmila Tomovska:** Conceptualization, Funding acquisition, Methodology, Project administration, Supervision, Validation, Writing – review & editing.

Declaration of competing interest

The authors declare that they have no known competing financial interests or personal relationships that could have appeared to influence the work reported in this paper.

Data availability

Data will be made available on request.

Acknowledgements

The authors would like to acknowledge the financial support provided by the Industrial Liaison Program in Polymerization in Dispersed Media (Akzo Nobel, Allnex, Arkema, BASF, Covestro, Elix Polymers, Innovyn, IQLIT, Organik Kimya, Sherwin Williams, Stahl, Synthomer, Tesa, Vinavil, and Wacker) and the Sgiker Services of University of the Basque Country. The author also acknowledge the funding from Basque Government (Project IT-1512-22).

Appendix A. Supplementary data

Supplementary data to this article can be found online at https://doi.org/10.1016/j.reactfunctpolym.2024.105843.

References

[1] B.L. Leigh, E. Cheng, L. Xu, A. Derk, M.R. Hansen, C.A. Guymon, Antifouling photograftable zwitterionic coatings on PDMS substrates, Langmuir 35 (2018) 1100–1110.
[2] Q. Shao, S. Jiang, Molecular understanding and design of zwitterionic materials, Adv. Mater. 27 (2015) 15–26.
[3] Z. Zhang, J.A. Finlay, L. Wang, Y. Gao, J.A. Callow, M.E. Callow, S. Jiang, Polysulfobetaine-grafted surfaces as environmentally benign ultralow fouling marine coatings, Langmuir 25 (2009) 13516–13521.
[4] W.K. Cho, B. Kong, I.S. Choi, Highly efficient non-biofouling coating of zwitterionic polymers: poly ((3-(methacryloylamino) propyl)-dimethyl (3-sulfopropyl) ammonium hydroxide), Langmuir 23 (2007) 5678–5682.
[5] M. Harijan, M. Singh, Zwitterionic polymers in drug delivery: a review, J. Mol. Recognit. 35 (2022) e2944.
[6] M. He, K. Gao, L. Zhou, Z. Jiao, M. Wu, J. Cao, X. You, Z. Cai, Y. Su, Z. Jiang, Zwitterionic materials for antifouling membrane surface construction, Acta Biomater. 40 (2016) 142–152.
[7] P. Bengani, Y. Kou, A. Asatekin, Zwitterionic copolymer self-assembly for fouling resistant, high flux membranes with size-based small molecule selectivity, J. Membr. Sci. 493 (2015) 755–765.
[8] S. Chen, L. Li, C. Zhao, J. Zheng, Surface hydration: principles and applications toward low-fouling/nonfouling biomaterials, Polymer 51 (2010) 5283–5293.

[9] T. Morisaku, J. Watanabe, T. Konno, M. Takai, K. Ishihara, Hydration of phosphorylcholine groups attached to highly swollen polymer hydrogels studied by thermal analysis, Polymer 49 (2008) 4652–4657.
[10] J. Wu, S. Chen, Investigation of the hydration of nonfouling material poly (ethylene glycol) by low-field nuclear magnetic resonance, Langmuir 28 (2012) 2137–2144.
[11] A. Rakovsky, D. Marbach, N. Lotan, Y. Lanir, Poly (ethylene glycol)-based hydrogels as cartilage substitutes: synthesis and mechanical characteristics, J. Appl. Polym. Sci. 112 (2009) 390–401.
[12] Z. Zhang, T. Chao, S. Chen, S. Jiang, Superlow fouling sulfobetaine and carboxybetaine polymers on glass slides, Langmuir 22 (2006) 10072–10077.
[13] Z.G. Estephan, P.S. Schlenoff, J.B. Schlenoff, Zwitteration as an alternative to PEGylation, Langmuir 27 (2011) 6794–6800.
[14] J. Ladd, Z. Zhang, S. Chen, J.C. Hower, S. Jiang, Zwitterionic polymers exhibiting high resistance to nonspecific protein adsorption from human serum and plasma, Biomacromolecules 9 (2008) 1357–1361.
[15] M. Li, B. Zhuang, J. Yu, Functional zwitterionic polymers on surface: structures and applications, Chemistry–An Asian Journal 15 (2020) 2060–2075.
[16] L. Wu, J. Jasinski, S. Krishnan, Carboxybetaine, sulfobetaine, and cationic block copolymer coatings: a comparison of the surface properties and antibiofouling behavior, J. Appl. Polym. Sci. 124 (2012) 2154–2170.
[17] E. Schönemann, J. Koc, J.F. Karthäuser, O. Özcan, D. Schanzenbach, L. Schardt, A. Rosenhahn, A. Laschewsky, Sulfobetaine methacrylate polymers of unconventional polyzwitterion architecture and their antifouling properties, Biomacromolecules 22 (2021) 1494–1508.
[18] T. Wang, X. Wang, Y. Long, G. Liu, G. Zhang, Ion-specific conformational behavior of polyzwitterionic brushes: exploiting it for protein adsorption/desorption control, Langmuir 29 (2013) 6588–6596.
[19] X. Jin, J. Yuan, J. Shen, Zwitterionic polymer brushes via dopamine-initiated ATRP from PET sheets for improving hemocompatible and antifouling properties, Colloids Surf. B Biointerfaces 145 (2016) 275–284.
[20] M.R. Hibbs, B.A. Hernandez-Sanchez, J. Daniels, Y.S.J. Stafslien, Polysulfone and polyacrylate-based zwitterionic coatings for the prevention and easy removal of marine biofouling, Biofouling 31 (2015) 613–624.
[21] D.K. Yeon, S. Ko, S. Jeong, S.-P. Hong, S.M. Kang, W.K. Cho, Oxidation-mediated, zwitterionic polydopamine coatings for marine antifouling applications, Langmuir 35 (2018) 1227–1234.
[22] S. Murali, A. Agirre, R. Tomovska, Zwitterionic monomers as stabilizers for high solids content polymer colloids for high-performance coatings applications, Prog. Org. Coat. 173 (2022) 107196.
[23] F. Polzer, J. Heigl, C. Schneider, M. Ballauff, O.V. Borisov, Synthesis and analysis of zwitterionic spherical polyelectrolyte brushes in aqueous solution, Macromolecules 44 (2011) 1654–1660.
[24] E. Aramendia, J. Mallégol, C. Jeynes, M.J. Barandiaran, J.L. Keddie, J.M. Asua, Distribution of surfactants near acrylic latex film surfaces: a comparison of conventional and reactive surfactants (surfmers), Langmuir 19 (2003) 3212–3221.
[25] N. Shirakbari, M. Ebrahimi, H. Salehi-Mobarakeh, M. Khorasani, Effect of surfactant type and concentration on surfactant migration, surface tension, and adhesion of latex films, Journal of Macromolecular Science, Part B 53 (2014) 1286–1292.
[26] M. Argaiz, F. Ruipérez, M. Aguirre, R. Tomovska, Ionic inter-particle complexation effect on the performance of waterborne coatings, Polymers 13 (2021) 3098.
[27] O. Azzaroni, A.A. Brown, W.T.S. Huck, UCST wetting transitions of polyzwitterionic brushes driven by self-association, Angew. Chem. Int. Ed. 45 (2006) 1770–1774.
[28] D. Howell, B. Behrends, A review of surface roughness in antifouling coatings illustrating the importance of cutoff length, Biofouling 22 (2006) 401–410.
[29] S. Guo, D. Jańczewski, X. Zhu, R. Quintana, T. He, K.G. Neoh, Surface charge control for zwitterionic polymer brushes: tailoring surface properties to antifouling applications, J. Colloid Interface Sci. 452 (2015) 43–53.
[30] H. Tang, T. Cao, X. Liang, A. Wang, S.O. Salley, J. McAllister, K.S. Ng, Influence of silicone surface roughness and hydrophobicity on adhesion and colonization of Staphylococcus epidermidis, Journal of Biomedical Materials Research Part A 88 (2009) 454–463.
[31] M. Herzberg, A. Sweity, M. Brami, Y. Kaufman, V. Freger, G. Oron, S. Belfer, R. Kasher, Surface properties and reduced biofouling of graft-copolymers that possess oppositely charged groups, Biomacromolecules 12 (2011) 1169–1177.
[32] X. Yu, J. Zhao, C. Wu, B. Li, C. Sun, S. Huang, X. Tian, Highly durable antifogging coatings resistant to long-term airborne pollution and intensive UV irradiation, Mater. Des. 194 (2020) 108956.
[33] G. Rong, D. Zhou, X. Han, J. Pang, Preparation and characterization of novel zwitterionic poly (arylene ether sulfone) ultrafiltration membrane with good thermostability and excellent antifouling properties, Appl. Surf. Sci. 427 (2018) 1065–1075.
[34] K. He, H. Duan, G.Y. Chen, X. Liu, W. Yang, D. Wang, Cleaning of oil fouling with water enabled by zwitterionic polyelectrolyte coatings: overcoming the imperative challenge of oil–water separation membranes, ACS Nano 9 (2015) 9188–9198.